IOP Publishing Nanotechnology
Nanotechnology 27 (2016) 225201 (6pp) doi:10.1088/0957-4484/27/22/225201

High performance MoS_2-based field-effect transistor enabled by hydrazine doping

Dongsuk Lim[1], E S Kannan[2], Inyeal Lee[1], Servin Rathi[1], Lijun Li[1], Yoontae Lee[1], Muhammad Atif Khan[1], Moonshik Kang[1,3], Jinwoo Park[1] and Gil-Ho Kim[1]

[1] School of Electronic and Electrical Engineering and Sungkyunkwan Advanced Institute of Nanotechnology (SAINT), Sungkyunkwan University, Suwon 16419, Korea
[2] Department of Physics, BITS-PILANI, K. K. BIRLA Goa Campus, Zuarinagar, Goa 403726, India
[3] Manufacturing Engineering Team, Memory Division, Samsung Electronics Co., Hwasung 18396, Korea

E-mail: ghkim@skku.edu

Received 2 December 2015, revised 29 March 2016
Accepted for publication 31 March 2016
Published 21 April 2016

Abstract

We investigated the n-type doping effect of hydrazine on the electrical characteristics of a molybdenum disulphide (MoS_2)-based field-effect transistor (FET). The threshold voltage of the MoS_2 FET shifted towards more negative values (from −20 to −70 V) on treating with 100% hydrazine solution with the channel current increasing from 0.5 to 25 μA at zero gate bias. The inverse subthreshold slope decreased sharply on doping, while the ON/OFF ratio increased by a factor of 100. Gate–channel coupling improved with doping, which facilitates the reduction of channel length between the source and drain electrodes without compromising on the transistor performance, making the MoS_2-based FET easily scalable.

Keywords: transition metal dichalcogenides, MoS_2, doping, field-effect transistor

(Some figures may appear in colour only in the online journal)

1. Introduction

There has been recent interest in transition metal dichalcogenide (TMDC)-based two-dimensional (2D) materials such as molybdenum disulphide (MoS_2) due to their excellent electrical, chemical, thermal and mechanical properties [1–4]. Their non-zero band gap makes them attractive for fabricating nanoscale transistors with a high ON/OFF ratio [5]. Another exciting possibility MoS_2 offers is the easy tunability of its electrical and optical properties by varying its thickness and adding dopants. Using MoS_2 flakes of different thickness, the energy band gap, phonon modes and optical absorption spectrum can be easily engineered according to the device requirements [6–9]. Considerable improvement in electron transport properties, gas and optical absorption characteristics and transistor characteristics were observed on doping the MoS_2 flakes [10–13]. More research is currently being done to achieve stable dopant incorporation, since the 2D nature of MoS_2 favors doping only by surface adsorption, which is very susceptible to degradation on exposure to ambient environment. Even though stability was achieved by substitutional doping, it degraded the mobility due to the defects caused by lattice distortion [14]. Therefore it is important to formulate a stable doping technique without compromising on the intrinsic properties of MoS_2.

MoS_2 is intrinsically n-type in its native form [15]. Several experimental and theoretical investigations provide contradictory evidence about the role of impurities (rhenium) and defects (sulphur vacancies) in the observed n-type conductivity of MoS_2 [16–18]. It is however clear from those studies that donor sites lie close to the valence band maximum, and the n-type conductivity is due to the activation of electrons from these shallow donor sites. At room temperature, carrier activation from the donor sites is very poor and conduction occurs mostly by the hopping mechanism [19]. Attempts to remove the MoS_2 defects with a chemical reaction showed improvement in the conductivity of MoS_2 [20]. Another method to improve the conduction in MoS_2 is to activate carriers by using electrostatic gates. Although the technique improved the conductivity of the channel, the current density was still too small for practical application [21]. There have been several attempts to overcome this

bottleneck by doping MoS_2 flakes with various donor species such as benzyl viologen, potassium and nitrogen dioxide [22–24]. All of these donor species except benzyl viologen were found to be highly unstable on exposure to air. Air-stable benzyl viologen showed great promise in controlling the doping in MoS_2 flakes but it requires a post-doping treatment with toluene to control the hydrazine concentration. This process is time-consuming and does not allow precise control over transport parameters of MoS_2 flakes, which is crucial for any device application.

In this work, we report on a very stable doping technique to tailor the transport properties of MoS_2 flakes using hydrazine. We show the stability of our doping technique by exposing the doped MoS_2 field-effect transistor (FET) to ambient environment (temperature 293 K) for weeks and examined the channel current in the device. Moreover, we were able to vary the carrier density and mobility of the material with ease by exposing MoS_2 to different concentration levels of hydrazine. We also show that the doping improved the performance and the ON/OFF ratio of the MoS_2-based FET.

2. Experimental details

The MoS_2 sample used for this study was micromechanically exfoliated using Scotch tape and transferred onto silicon substrate (heavily n-doped) with 285-nm-thick silicon dioxide. On this layer, electrode patterns were fabricated by photo-lithography, and using electron-beam evaporation 10-nm-thick Ti and 60 nm thick Au were deposited for making contacts with a low Schottky barrier. After lift-off using acetone, the resulting structure is a three-terminal MoS_2 FET, a schematic diagram of which is shown in figure 1(a). To determine the thickness of the exfoliated MoS_2 layers, it was first identified using an optical microscope and characterized using Raman spectroscopy. Figure 1(b) shows the Raman spectrum of the MoS_2, which was taken at room temperature using a 532 nm laser. From the observed difference of 24 cm^{-1} between the Raman peaks, which corresponds to in-plane and out-of-plane vibrational modes (E^1_{2g} and A_{1g}), the thickness of the flakes can be approximated to be around 3–4 layers [7]. The device was then exposed to hydrazine solution of varying concentrations (0.1% to 100%) for 30 s. This hydrazine doping process has also been studied on various 2D materials such as graphene [25] and WSe_2 [26]. After treatment, the intensity of the Raman peak was found to decrease due to dopant incorporation. There is, however, no change in the position of the Raman peak, an indication that there is no distortion in the crystal lattice due to hydrazine treatment, and all the inherent vibrational modes of MoS_2 remain intact [25, 27]. The concentration of hydrazine is represented in the units of volume percentage. 100% corresponds to a pure hydrazine solution and a 10% solution contains 3 ml hydrazine in 27 ml de-ionized water.

For studying transistor characteristics, the heavily n-doped silicon substrate was used as a back-gate to modulate

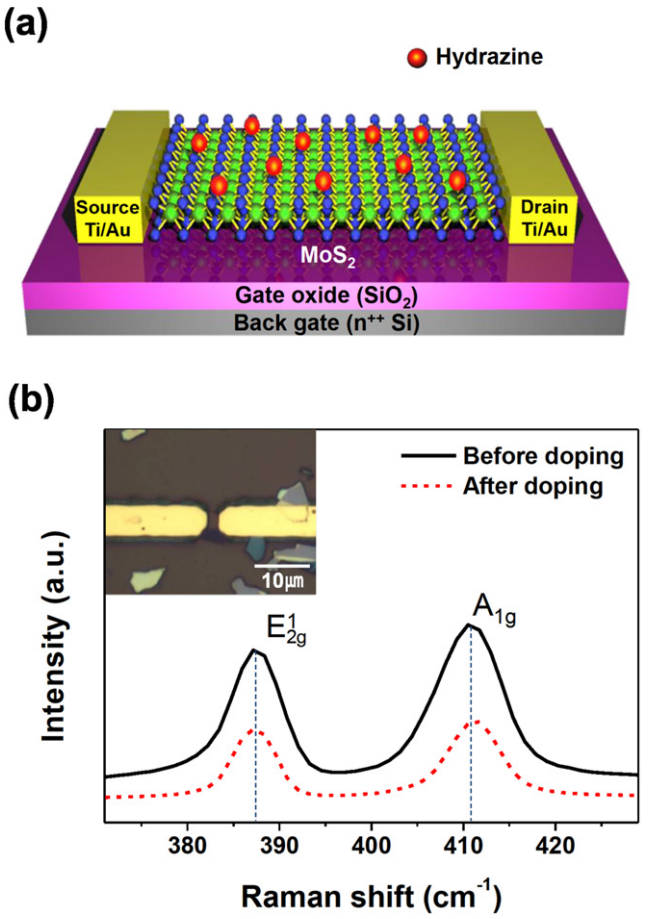

Figure 1. (a) Schematic diagram showing the view of the MoS_2 FET structure. (b) Room temperature Raman spectra of MoS_2 using 532 nm laser. The inset shows an optical microscope image of the device.

the carrier density, the source contact was grounded, and the drain contact was biased with a positive and negative voltage. To study the effectiveness of hydrazine as a dopant, the MoS_2 FET was treated with hydrazine solution of varying concentrations from 0.1% to 100%. All the doping trials were carried out on a single MoS_2 device to avoid the inherent device-to-device variability. The transistor characteristics were first studied in a MoS_2 FET treated with 0.1% hydrazine solution. It was then cleaned with de-ionized water (hydrazine is readily soluble in water) and blow-dried using nitrogen gas. After this cleaning process, the sample returned to its native state. The cleaned sample was then repeatedly exposed to hydrazine solution of varying concentrations and the same cleaning procedure was followed after every exposure. The transport properties were then studied after each exposure to optimize the hydrazine concentration for better transistor performance. We also investigated the doping efficiency of 100% hydrazine solution by varying the exposure time.

3. Results and discussion

Figure 2(a) shows the current–voltage characteristics (I_d–V_d) of MoS_2 FET treated with hydrazine solution of different

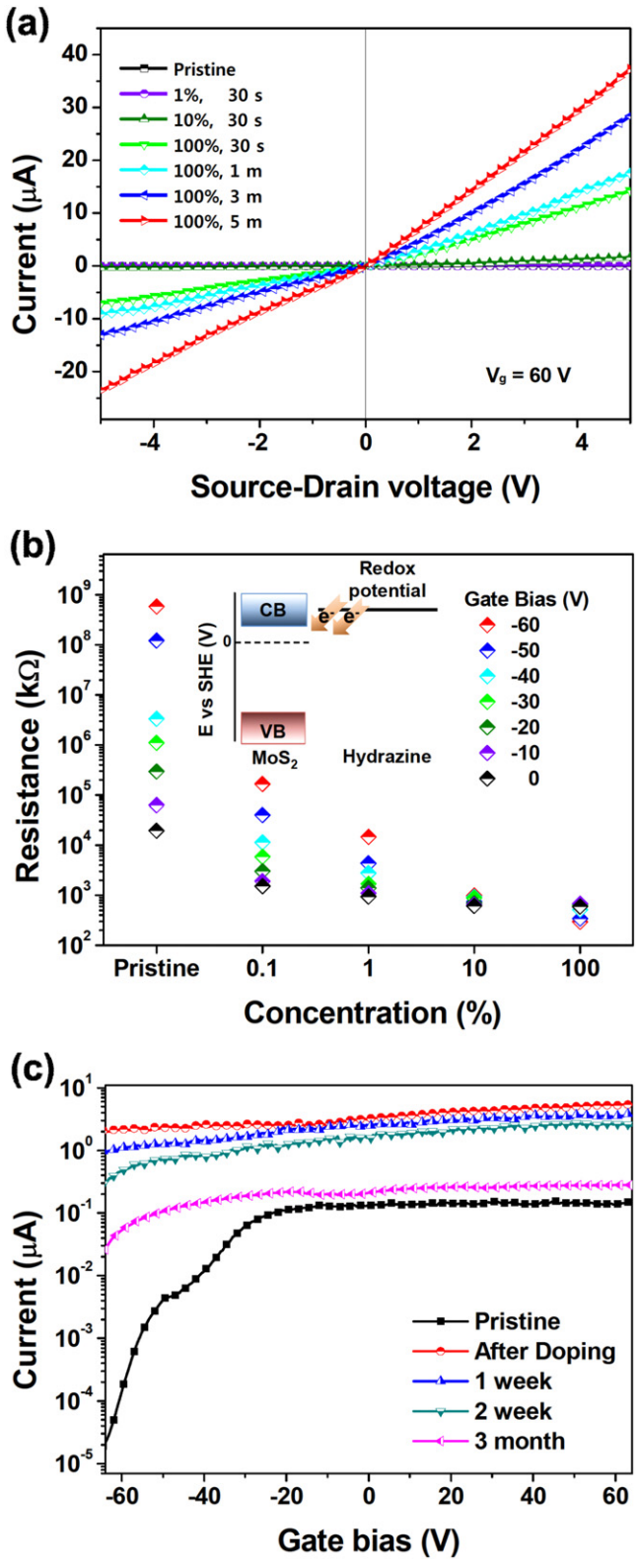

Figure 2. (a) Output characteristics of current–voltage with various hydrazine doping concentrations and treatment times with back-gate voltage of 60 V. (b) Resistance as a function of varying concentrations for different gate voltages. Inset image shows energy band diagram of MoS_2 and hydrazine redox states. (c) I_d–V_g characteristics of hydrazine-doped MoS_2 FET for different time intervals.

concentrations for a time period of 30 s. A back-gate voltage of 60 V was applied to ensure sufficient carrier population in the channel. It is very clear from figure 2(a) that hydrazine treatment improved the channel conductance significantly. I_d–V_d characteristics bear the signature of n-type doping with resistance dropping on increasing the concentration of hydrazine used for treatment. Further confirmation of n-type doping was determined from the field-effect studies of the hydrazine-doped MoS_2 transistors by changing the gate bias from −60 to 0 V (figure 2(b)). Our device has a higher operating voltage due to the large thickness of the gate dielectric, which is around 300 nm. The operating voltage can be decreased by fabricating a top-gated transistor using a high k dielectric as reported recently by Changjian *et al* [28]. On increasing the gate voltage the channel resistance decreased considerably for pristine MoS_2 and moderately for lightly doped MoS_2 (0.1 and 1%). In the case of highly doped MoS_2 (10 and 100%) samples, the variation in channel resistance with V_g is very small. In samples treated with a high concentration of hydrazine (100%), the electron density was so high that it required a larger electric field for carrier modulation and the channel current practically remained constant irrespective of the changes in the gate voltage (figure 2(b)).

The doping mechanism of hydrazine can be explained by the dipole–dipole interaction between the MoS_2 surface and hydrazine molecule [28–30]. The dipole–dipole interaction between the facile dopant and 2D semiconductor can be explained on the basis of energy level offset between the conduction band (CB) edge and reduction potential of hydrazine [19]. Energy level offset between the CB of MoS_2 and redox potential of hydrazine, as illustrated in the inset of figure 2(b), results in a charge transfer (electron) from hydrazine to MoS_2 and consequently, the n-doped MoS_2 layer is achieved [31, 32]. As a result of n-doping in the MoS_2 layer, there is a drastic improvement in the device characteristics due to a decrease in the Schottky barrier height at the interface of the MoS_2/Ti metal contact [22, 33]. This highly conducting MoS_2 transistor function can be used in digital circuits where external voltage needs to be applied to turn off the device, and the channel is always ON for $V_g = 0$V The doping effect was found to be stable even after long exposure to ambient conditions (figure 2(c)). This indicates a strong interaction between the hydrazine molecule and the MoS_2 surface. On examining the doping stability after 3 months, a slight decrease in the n-doping level was observed. This may be due to the replacement of hydrazine molecules with oxygen from the ambient environment and the slow spontaneous desorption of hydrazine from the MoS_2 surface. Our doping technique can be combined with the recently demonstrated p-doping technique on MoS_2 by Suh *et al* for fabricating TMD-based circuits for digital electronics [14].

One of the major disadvantages in using pristine MoS_2 FETs is that the ON current is very small (0.5 μA) at zero gate bias, which may lead to severe noise-related issues. Figures 3(a) and (b) show the current in linear and logarithm

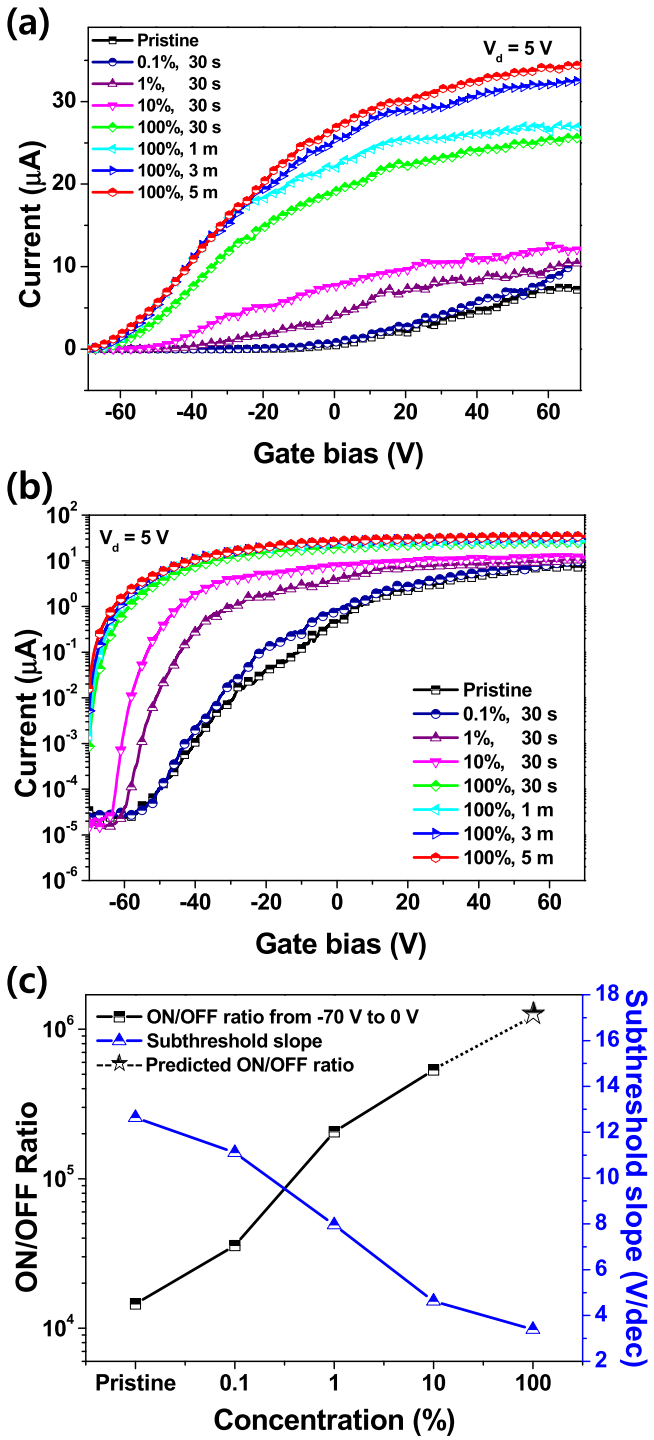

Figure 3. (a) Transfer characteristics (I_d–V_g) with various concentrations and treatment times of hydrazine solution with source–drain voltage of 5 V (b) and the corresponding log scale plot. (c) ON/OFF ratio (OFF state at −70 V and ON state at 0 V) and subthreshold slope of the MoS_2 FET with various concentrations of hydrazine. The dotted line between 10 and 100% treatment indicates the predicted ON/OFF ratio as the gate sweep in this case was restricted by the dielectric breakdown limit.

scale as a function of gate bias, respectively. In doped samples at 100% concentration, the ON current at zero gate bias is around 25 μA, which is two orders of magnitude greater than the pristine sample. The enhanced current density in the ON state is particularly attractive for high power applications. As the hydrazine concentration is increased from 0% to 100%, the threshold voltage (V_{th}) shifted from −20 to −70 V for 30 s exposure time. No significant change in V_{th} and channel current was observed on increasing the exposure time in 100% hydrazine-treated samples. It shows that the hydrazine is a very efficient donor species and interacts quickly with MoS_2 layers. The ability to tune V_{th} by doping offers the unique advantage of customizing the transistor performance according to our requirements. For instance, in digital circuits requiring high ON current, a MoS_2 FET with high V_{th} (100% hydrazine-treated sample) can be used, and low V_{th} samples can be used in those circuits requiring lower ON current [34].

In samples with high V_{th} the inverse subthreshold slope (equation (1)) shifted from 13 to 3 V/dec. The subthreshold slope is significantly lower (sharp transition from OFF to ON state) indicating that the gate has better control over the channel current (figure 3(c)):

$$S = \partial V_g / \partial(\log I_d) \tag{1}$$

This in turn improved the ON/OFF ratio by a factor of 100 and the magnitude did not change on varying the source–drain bias. It shows that with doping, the electrostatic effects of the source and drain electrodes on the channel decrease, and the gate-to-channel coupling increases. This is very important for the scalability of MoS_2-based transistors, as the gate electrode will be able to control the potential distribution and flow of current in the channel even when the channel length between the source and drain electrodes is decreased.

In our study the charge transfer doping technique improves the mobility by increasing the carrier concentration of the MoS_2 layer and subsequently lowering the channel resistance. Other physical parameters such as impurity scattering, defect scattering and phonon scattering that affect the mobility of the MoS_2 layer remain largely unaffected by hydrazine treatment. Figures 4(a) and (b) show the mobility and carrier density as a function of hydrazine concentration. In general, with the addition of dopant, the mobility increases first and then decreases as the scattering due to impurities dominates at high doping concentrations. In this case, both the parameters increased monotonically with hydrazine concentration, confirming the n-type doping effect of hydrazine. This is due to the effect of channel conductance dominating over impurity scattering in the electron transport. Conductance is directly proportional to the concentration of electrons in the conduction band. It is a clear indication that the increase in channel current with doping is mainly due to the increment in carrier concentration.

Field-effect mobility (μ) is calculated using the formula

$$\mu = \left[\frac{dI_d}{dV_g}\right] \times \left(\frac{L}{WC_{ox}V_d}\right) \tag{2}$$

where dI_d/dV_g is the slope of figure 3(b), L/W is the length to width ratio of the channel, C_{ox} is the capacitance of the oxide layer and V_d is the source–drain bias. The effect of contact resistance on the transport properties of the MoS_2 FET is

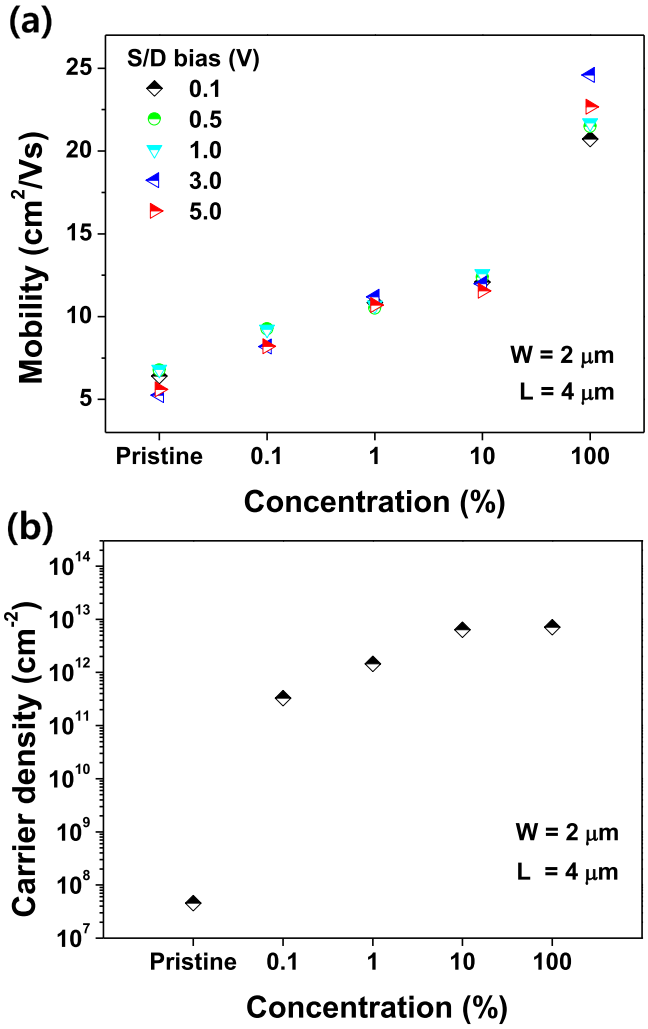

Figure 4. (a) Field-effect mobility and (b) carrier density as a function of concentration.

negligible as the metal–MoS_2 junction has a low Schottky barrier [35, 36]. So by a good approximation, we can exclude the effect of contact resistance on the field-effect mobility of the MoS_2 FET. Enhancement in the field-effect mobility in doped samples indicates that the conduction now occurs mainly by drift rather than hopping, as in the case of the pristine sample. As a result, the resistance of the channel decreased considerably with doping and the mobility of the device increased. From the calculated value of μ, the carrier density (n) is determined using the formula

$$n = 1/\mu\rho e \tag{3}$$

where ρ is the resistivity of the channel and e is the charge of the electron. The carrier density in MoS_2 increased almost by a factor of 6 from 10^7 to $10^{12}\,cm^{-2}$ on treating the pristine sample with 100% hydrazine.

4. Conclusion

In conclusion, we investigated the effectiveness and stability of hydrazine as an n-type dopant and its influence on the transistor characteristics of MoS_2-based FETs. Hydrazine bonded very quickly (30 s) with MoS_2 in ambient conditions. Mobility increased substantially on doping, with the density of carriers increasing almost by 10^6. Hydrazine doping increased the ON current in MoS_2 FETs and enhanced the switching speed by reducing the inverse subthreshold slope. The ON/OFF ratio increased by two orders of magnitude with doping, while also enhancing the gate–channel coupling. Therefore, hydrazine-doped MoS_2 is an ideal candidate for nanoscale digital electronics as it allows scaling of TMDC-based transistors to smaller dimensions.

Acknowledgments

This research was supported by the Basic Science Research Program through the National Research Foundation of Korea (NRF) funded by the Ministry of Education, Science and Technology (2013R1A2A2A01069023, 2014K2A2A4001415 and 2015H1D3A1062519).

References

[1] Kuc A, Zibouchse N and Heine T 2011 Influence of quantum confinement on the electronic structure of the transition metal sulfide TS_2 *Phys. Rev.* B **83** 245213
[2] Ghorbani-Asl M, Borini S, Kuc A and Heine T 2013 Strain-dependent modulation of conductivity in single-layer transition-metal dichalcogenides *Phys. Rev.* B **87** 235434
[3] Mak K F, Lee C, Hone J, Shan J and Heinz T F 2010 Atomically thin MoS_2: a new direct-gap semiconductor *Phys. Rev. Lett.* **105** 136805
[4] Zhang S L, Choi H H, Yue H Y and Yang W C 2014 Controlled exfoliation of molybdenum disulfide for developing thin film humidity sensor *Curr. Appl. Phys.* **14** 264–8
[5] Kim S *et al* 2012 High-mobility and low-power thin-film transistors based on multilayer MoS_2 crystals *Nat. Commun.* **3** 1011
[6] Lee C, Yan H, Brus L E, Heinz T F, Hone J and Ryu S 2010 Anomalous lattice vibrations of single- and few-layer MoS_2 *ACS Nano* **4** 2695–700
[7] Ye M, Winslow D, Zhang D, Pandey R and Yap Y K 2015 Recent advancement on the optical properties of two-dimensional molybdenum disulfide (MoS_2) thin films *Photonics* **2** 288–307
[8] Frindt R F 1965 Optical absorption of a few unit-cell layers of MoS_2 *Phys. Rev.* **140** A536–9
[9] Chuang S *et al* 2014 MoS2 P-type Transistors and diodes enabled by high work function MoO_x contacts *Nano Lett.* **14** 1337–42
[10] Mouri S, Miyauchi Y and Matsuda K 2013 Tunable photoluminescence of monolayer MoS_2 via chemical doping *Nano Lett.* **13** 5944–8
[11] Tarasov A, Zhang S, Tsai M, Campbell P M, Graham S, Barlow S, Marder S R and Vogel E M 2015 Controlled doping of large-area trilayer MoS2 with molecular reductants and oxidants *Adv. Mater.* **27** 1175–81
[12] Perkins F K, Friedman A L, Cobas E, Campbell P M, Jernigan G G and Jonker B T 2013 Chemical vapor sensing with monolayer MoS_2 *Nano Lett.* **13** 668–73
[13] Nipane A, Karmakar D, Kaushik N, Karande S and Lodha S 2016 Few-layer MoS2 p-type devices enabled by selective

doping using low energy phosphorus implantation *ACS Nano* **10** 2128
[14] Suh J *et al* 2014 Doping against the native propensity of MoS_2: degenerate hole doping by cation substitution *Nano Lett.* **14** 6976–82
[15] Qiu H *et al* 2013 Hopping transport through defect-induced localized states in molybdenum disulphide *Nat. Commun.* **4** 2642
[16] Noh J Y, Kim H and Kim Y S 2014 Stability and electronic structures of native defects in single-layer MoS_2 *Phys. Rev.* B **89** 205417
[17] Ugeda M M *et al* 2014 Giant bandgap renormalization and excitonic effects in a monolayer transition metal dichalcogenide semiconductor *Nat. Mater.* **13** 1091–5
[18] Komsa H P and Krasheninnikov A V 2015 Native defects in bulk and monolayer MoS2 from first principles *Phys. Rev.* B **91** 125304
[19] Lo S T, Klochan O, Liu C H, Wang W H, Hamilton A R and Liang C T 2014 Transport in disordered monolayer MoS2 nanoflakes evidence for inhomogeneous charge transport *Nanotechnology* **25** 375201
[20] Yu Z *et al* 2014 Towards intrinsic charge transport in monolayer molybdenum disulfide by defect and interface engineering *Nat. Commun.* **5** 5290
[21] Chu L, Schmidt H, Pu J, Wang S, Özyilmaz B, Takenobu T and Eda G 2014 Charge transport in ion-gated mono, bi, and trilayer MoS_2 field effect transistors *Sci. Rep.* **4** 7293
[22] Kiriya D, Tosun M, Zhao P, Kang J S and Javey A 2014 Air stable surface charge transfer doping of MoS_2 by Benzyl viologen *J. Am. Chem. Soc.* **136** 7853–6
[23] Fang H, Chuang S, Chang T C, Takei K, Takahashi T and Javey A 2012 High performance single layered WSe_2 p-FETs with chemically doped contacts *Nano Lett.* **12** 3788–92
[24] Fang H, Tosun M, Seol G, Chang T C, Takei K, Guo J and Javey A 2013 Degenerate n-doping of few-layer transition metal dichalcogenides by potassium *Nano Lett.* **13** 1991–5
[25] Lee I Y, Park H Y, Park J H, Lee J, Jung W S, Yu H Y, Kim S W, Kim G H and Park J H 2013 Hydrazine based n-type doping process to modulate Dirac point of graphene and its application to complementary inverter *Org. Electron.* **14** 1586–90
[26] Lee I Y, Rathi S, Li L, Lim D S, Khan M A, Kannan E S and Kim G H 2015 Non-degenerate n-type doping by hydrazine treatment in metal work function engineered WSe_2 field-effect transistor *Nanotechnology* **26** 255203
[27] Dhakal K P, Duong D L, Lee J, Nam H, Kim M, Kan M, Lee Y H and Kim J 2014 Confocal absorption spectral imaging of MoS_2: optical transitions depending on the atomic thickness of intrinsic and chemically doped MoS_2 *Nanoscale* **6** 13028–35
[28] Changjian W, Xinsheng R, Salahuddin L, Ziyuan V, Daniel H, Baoling C H, Lai-Wa C and Mansun C Y 2015 Low voltage and high ON/OFF ratio field-effect transistors based on CVD MoS2 and ultra high-k gate dielectric PZT *Nanoscale* **7** 8695–700
[29] Komsa H P, Kurasch S, Lehtinen O, Kaiser U and Krasheninnikov A V 2013 From point to extended defects in two-dimensional MoS_2: evolution of atomic structure under electron irradiation *Phys. Rev.* B **88** 035301
[30] Han Y, Hu T, Li R, Zhoub J and Dong J 2015 Stabilities and electronic properties of monolayer MoS_2 with one or two sulfur line vacancy defects *Phys. Chem. Chem. Phys.* **17** 3813–9
[31] Frost R L, Kristof J, Horvath E and Martens W N 2002 Complexity of intercalation of hydrazine into kaolinite a controlled rate thermal analysis and drift spectroscopic study *J. Colloid Interface Sci.* **251** 350–9
[32] Schlaf R, Lang O, Pettenkofer C and Jaegermann W 1999 Band lineup of layered semiconductor heterointerfaces prepared by van der Waals epitaxy: charge transfer correction term for the electron affinity rule *Appl. Phys. Lett.* **85** 2732–53
[33] Goia D V and Matijevic E 1998 Preparation of monodispersed metal particles *New J. Chem.* **22** 1203–15
[34] Rai A *et al* 2015 Air stable doping and intrinsic mobility enhancement in monolayer molybdenum disulfide by amorphous titanium suboxide encapsulation *Nano Lett.* **15** 4329–36
[35] Khatami Y and Banerjee K 2009 Steep subthreshold slope n- and p-type tunnel-FET devices for low-power and energy-efficient digital circuits *IEEE Trans. Electron Devices* **56** 2752–61
[36] Yang L *et al* 2014 Chloride molecular doping technique on 2D materials: WS_2 and MoS_2 *Nano Lett.* **14** 6275–80